LIMNOLOGY and OCEANOGRAPHY

ASLO

Limnol. Oceanogr. 65, 2020, S310–S320

doi: 10.1002/lno.11310

Distribution of mercury-cycling genes in the Arctic and equatorial Pacific Oceans and their relationship to mercury speciation

Katlin L. Bowman,[1*] **R. Eric Collins**,[2] **Alison M. Agather**,[3] **Carl H. Lamborg**,[1] **Chad R. Hammerschmidt**,[3] **Drishti Kaul**,[4] **Christopher L. Dupont**,[4] **Geoff A. Christensen**,[5] **Dwayne A. Elias**[5]

[1]Department of Ocean Sciences, University of California Santa Cruz, Santa Cruz, California
[2]College of Fisheries & Ocean Sciences, University of Alaska Fairbanks, Fairbanks, Alaska
[3]Department of Earth and Environmental Sciences, Wright State University, Dayton, Ohio
[4]Microbial and Environmental Genomics Department, J. Craig Venter Institute, La Jolla, California
[5]Biosciences Division, Oak Ridge National Laboratory, Oak Ridge, Tennessee

Abstract

Humans are exposed to potentially harmful amounts of the neurotoxin monomethylmercury (MMHg) through consumption of marine fish and mammals. However, the pathways of MMHg production and bioaccumulation in the ocean remain elusive. In anaerobic environments, inorganic mercury (Hg) can be methylated to MMHg through an enzymatic pathway involving the *hgcAB* gene cluster. Recently, *hgcA*-like genes have been discovered in oxygenated marine water, suggesting the *hgcAB* methylation pathway, or a close analog, may also be relevant in the ocean. Using polymerase chain reaction amplification and shotgun metagenomics, we searched for but did not find the *hgcAB* gene cluster in Arctic Ocean seawater. However, we detected Hg-cycling genes from the *mer* operon (including organomercury lyase, *merB*), and *hgcA*-like paralogs (i.e., *cdhD*) in Arctic Ocean metagenomes. Our analysis of Hg biogeochemistry and marine microbial genomics suggests that various microorganisms and metabolisms, and not just the *hgcAB* pathway, are important for Hg methylation in the ocean.

The concentration and fate of mercury (Hg) in the ocean is controlled by the distribution of four principal species: mercuric ion (Hg[II]), elemental Hg (Hg^0), monomethyl-Hg (CH_3Hg^+; MMHg), and dimethyl-Hg ($[CH_3]_2Hg$; DMHg). MMHg is a neurotoxin that bioaccumulates in marine food webs and humans are primarily exposed through consumption of coastal and open-ocean fish, and marine mammals (Debes et al. 2016; Madigan et al. 2018; Schartup et al. 2018; Sunderland et al. 2018). Except for the Indian Ocean, which remains untested, MMHg and DMHg have been detected in the water column of every ocean basin (Mason and Fitzgerald 1993; Mason et al. 1995; Sunderland et al. 2009; Cossa et al. 2011, 2018; Wang et al. 2012, 2018; Bowman et al. 2015, 2016; Heimbürger et al. 2015; Munson et al. 2015; Agather et al. In press). Furthermore, anthropogenic emissions have increased total Hg concentrations in the ocean since preindustrial times (Lamborg et al. 2014), suggesting the hypothesis that MMHg has increased as well. A detailed understanding of the reactions involved in the formation and destruction of MMHg in the ocean is imperative for testing this hypothesis.

The four principal species of Hg in the ocean are interconnected through abiotic reactions and enzymatic catalysis, but a detailed understanding of those reactions is lacking. Various bacterial and archaeal genomes encode the *mer* operon, which encodes a suite of enzymes that touch on Hg cycling in a variety of ways (Barkay et al. 2003; Boyd and Barkay 2012). For example, the *mer* operon includes genes that encode for an activator/repressor (MerR or ArsR) and periplasmic scavenging protein (MerP) responsive to Hg(II), transport proteins to shuttle Hg(II) (MerT, MerC, MerF, MerG) or MMHg (MerE) into bacterial cytoplasm, mercuric reductase (MerA) to reduce Hg(II) to Hg(0), and organomercury lyase (MerB) to de-methylate MMHg to Hg(II) (Brown et al. 2003; Busenlehner et al. 2003; Boyd and Barkay 2012). The prevalence of these genes in the ocean and their influence on ambient Hg cycling are poorly understood.

In anoxic environments, production of MMHg is associated with microbes containing *hgcA*, a gene that encodes for a methyltransferase enzyme that methylates Hg, apparently through the use of a cobalamin-containing cofactor (Parks et al. 2013). This gene, and its required ferredoxin-encoding partner *hgcB*, has been found in the genomes of diverse organisms and primarily in the sulfate- and iron-reducing bacteria and methanogenic archaea, dramatically widening the taxonomic range of organisms that

*Correspondence: klbowman@ucsc.edu

Additional Supporting Information may be found in the online version of this article.

Special Issue: Linking Metagenomics to Aquatic Microbial Ecology and Biogeochemical Cycles. Edited by: Hans-Peter Grossart, Ramon Massana, Katherine McMahon and David A. Walsh.

might be capable of methylating Hg (Gilmour et al. 2013; Parks et al. 2013). Furthermore, *hgcA* has been found in metagenomes from seawater, marine sediment, animal microbiota, and soils (Podar et al. 2015), suggesting that *hgcAB* genes may control Hg methylation in a wide variety of environmental settings.

Known *hgcAB* carriers are all obligate anaerobes, presenting a paradox for oceanic Hg methylation because anoxic conditions are rare in the pelagic zone. Methylation of Hg and demethylation of MMHg are known to occur in the marine water column (Monperrus et al. 2007; Lehnherr et al. 2011; Munson et al. 2018). Therefore, one or more of the following conditions is likely true: (1) methylation occurs in low-oxygen microenvironments such as inside suspended or sinking particles and aggregates, (2) *hgcAB* occurs in microbes that are not obligate anaerobes, or (3) methylation occurs through a pathway that does not involve *hgcAB*. The first possibility is supported by recent experimental and modeling work (Ortiz et al. 2015; Bianchi et al. 2018); however, when measured, sinking particles appear to be depleted in MMHg relative to phytoplankton biomass (Munson et al. 2015). The second and third possibilities remain to be tested. There is some indication that both might be true, as Podar et al. (2015) found *hgcA*-like sequences in the metagenomes of oxic water samples and Munson et al. (2018) found evidence for extracellular methylation of Hg.

To address these hypotheses, we investigated the presence of Hg-cycling genes (*hgcAB*, *mer*) as well as other functional genes associated with metal transport and methylation in microbial communities from seawater samples for which detailed Hg speciation measurements were also made. Here, we present new targeted gene amplification and metagenomics results from the western Arctic Ocean (2015 U.S. GEOTRACES GN01) and revisit metagenomic and Hg data from the equatorial North Pacific MetZyme expedition (Saito et al. 2014; Munson et al. 2015; Santoro et al. 2017).

Methods

Sample collection

Samples were collected aboard USCGC *Healy* during the U.S. Arctic GEOTRACES expedition from August 2015 to October 2015. The transect began in the Bering Strait, traversed north through the Makarov Basin to the North Pole and returned south through the Canada Basin to Dutch Harbor, Alaska. Locations sampled for DNA extraction and Hg analysis included the Bering Sea, Chukchi Sea, Makarov, and Canada Basins (Fig. 1). Seawater and particle sampling procedures followed that of previous US GEOTRACES cruises (e.g., Bowman et al. 2015, 2016; Agather et al. In press). In brief, seawater was collected in 12-liter Teflon-coated Go-Flo bottles deployed from a trace-metal clean rosette (Cutter and Bruland 2012), and filtered through prerinsed capsules (0.2 μm, Pall AcroPak-200) under clean laboratory conditions. Filtered water was purged of DMHg with Hg-free N_2 gas, transferred to 0.25-liter borosilicate glass bottles, acidified with 1% sulfuric acid, and shipped frozen to Wright State University for MMHg analysis.

Suspended particles (1–51 μm) and DNA were collected using McLane in situ pumps equipped with "mini-MULVFS" filter holders (Bishop et al. 2012; Lam et al. 2015). Quartz fiber filters loaded with suspended particles were frozen and transported to Wright State University for analysis of MMHg. Sterivex filters (0.22 μm, Millipore) were secured to an unmetered pump attachment (three filters per depth, 2–18 depths per station)

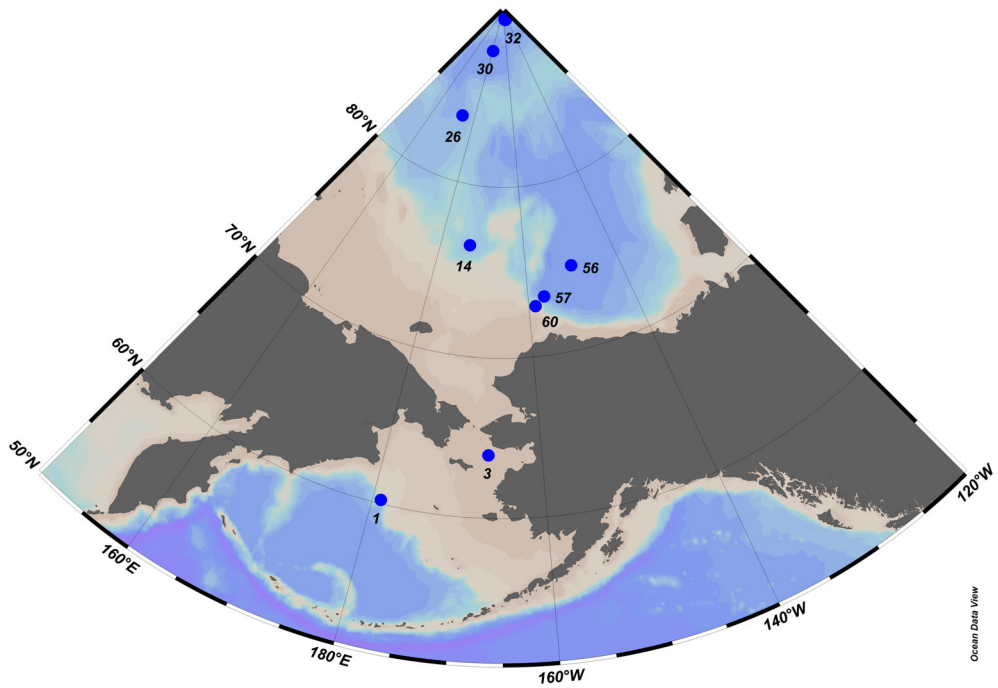

Fig. 1. Stations occupied during the 2015 U.S. GEOTRACES Arctic expedition (GN01) where samples for DNA extraction and Hg analysis were collected.

and immediately preserved with lysis buffer (Wright et al. 2009) following recovery of the McLane pumps. Preserved Sterivex filters were stored at −80°C on the ship, and transported on dry ice to University of California, Santa Cruz.

The upper water column (< 800 m) was sampled for DNA extraction and Hg analysis in the equatorial North Pacific Ocean during the MetZyme expedition in October 2011 (Sta. 3, 8°N 156°W; Saito et al. 2014; Munson et al. 2015; Santoro et al. 2017). Filtered water and suspended particles for MMHg analysis were collected and stored similarly to the Arctic expedition described above (Munson et al. 2015). DNA was collected on 0.2-μm Supor-200 filters (Pall) using McLane in situ pumps and stored at −80°C until analysis (Santoro et al. 2017).

Mercury analysis

Filtered and particulate MMHg was determined by direct ethylation for both Arctic and Pacific samples (Munson et al. 2015; Agather et al. In press). Acidified seawater was neutralized with KOH, buffered with acetate or citric acid, amended with ascorbic acid, derivatized with sodium tetraethylborate, and analyzed via flow injection gas chromatographic cold vapor atomic fluorescence spectrometry (GC-CVAFS; Tseng et al. 2004; Bowman and Hammerschmidt 2011; Munson et al. 2014). Particulate MMHg was analyzed by flow-injection GC-CVAFS following digestion in 2 mol L^{-1} HNO_3 for 12 h in a 60°C water bath (Munson et al. 2015; Agather et al. In press).

DNA extraction

Genomic DNA (gDNA) from the Arctic Ocean was extracted from Sterivex filters using a phenol-chloroform method described by Wright et al. (2009), and stored in TE buffer at −20°C. The presence of DNA in each extract (n = 193) was verified with universal 16S rRNA gene polymerase chain reaction (PCR) primers 8F and 1492R (Turner et al. 1999). gDNA was quantified with Qubit (Thermo Fisher Scientific) and sample purity was assessed with Nanodrop ND-1000 (Thermo Fisher Scientific). Absorbance ratios $A_{260/280}$ and $A_{260/230}$ averaged 1.60 ± 0.08 and 1.57 ± 0.23 (n = 193), respectively, indicating the presence of contaminants (e.g., phenol). However, successful verification of DNA with 16S rRNA gene primers suggested the sample matrix did not interfere with the PCR. Extractions yielded 10–10,000 ng of DNA per filter which was sufficient for both PCR and metagenomic analyses. DNA extraction from the equatorial North Pacific is detailed by Santoro et al. (2017).

PCR amplification

gDNA from the Arctic Ocean (excluding Sta. 60; n = 193) was tested for the presence of *hgcAB* with broad-range degenerate PCR primers and *hgcA* with clade-specific quantitative PCR (qPCR) primers following protocols from Christensen et al. (2016). DNA extracts from *Geobacter sulfurreducens* (ATCC 51573D-5), *Desulfitobacterium metallireducens* (DMS15288), and *Methanomethylovorans hollandica* (DMS15978), known methylators with the *hgcAB* gene cluster, were used as positive controls (https://www.atcc.org, https://www.dsmz.de). For PCR, Platinum *Taq* DNA polymerase (Invitrogen) was used in a 20 μL reaction with 1 μmol L^{-1} of forward primer ORNL-HgcAB-uni-F, 1 μmol L^{-1} reverse primer ORNL-HgcAB-uni-R, 1.5 mmol L^{-1} $MgCl_2$, 0.2 mmol L^{-1} dNTPs, 10 ng gDNA template, and 10^6 copies of a positive control. Reaction conditions from Christensen et al. (2016) were followed, with one exception: the initial denaturation temperature was lowered to 95°C. Amplification of 10^5 copies of *hgcAB* from *G. sulfurreducens* in gDNA template was achieved, indicating no matrix interference (n = 3). Amplicons that closely matched the positive control in size were extracted and purified from an agarose gel, cloned with TOPO TA Cloning Kit (Invitrogen), sequenced by the Sanger method (GENEWIZ), and translated to peptide sequences (EMBOSS Transeq) after removing vector contamination (VecScreen, www.ncbi.nlm.nih.gov). Nucleic acid sequences are provided as Supporting Information.

Clade-specific qPCR was performed for *Deltaproteobacteria*, *Firmicutes*, and *Archaea* using iTaq Universal SYBR Green (Bio Rad), 1 ng of gDNA template, and primers and reaction conditions from Christensen et al. (2016). The relative limit of detection (copies detected at 30 cycles) ranged from 50 to 680 copies of *hgcA*, average efficiency ($\%E = (10^{(-1/\text{slope})} - 1) \times 100$) was 77–86%, and average recovery of 10^4–10^5 copies of *hgcA* from gDNA extracts was 97–111% (Supporting Information Table S1).

Metagenomic analysis

Illumina MiSeq shotgun sequencing and metagenomic analysis was used to characterize gDNA from GEOTRACES Sta. 26 and 30 in the Makarov Basin, and Sta. 60 at the Chukchi shelf. Sequence data were assembled and annotated using the EBI Metagenomics Pipeline Version 4.0 (Mitchell et al. 2018). Metagenomic data for Sta. 3 in the equatorial North Pacific (MetZyme) were produced by the United States Department of Energy Joint Genome Institute (JGI; http://www.jgi.doe.gov/) using Illumina HiSeq 2000 or 2500 (Santoro et al. 2017). Hidden Markov model (HMM) profiles (Podar et al. 2015) were used to search for orthologs of *hgcA* and *hgcB* in the Arctic Ocean metagenome. In the equatorial North Pacific metagenome, *hgcA*-like genes were first identified by Podar et al. (2015). For both Arctic and Pacific metagenomes, taxonomic reads were normalized to 16S rRNA gene copy number estimated by *rrn*DB (Stoddard et al. 2015), and used to calculate relative abundance (i.e., taxonomic reads/cell in each sample). Functional genes were normalized to the total number of genes identified in each sample (13,000–1,234,083 genes per sample). Correlation coefficients were calculated using the Pearson product-moment correlation in SigmaPlot version 13.0. Shotgun metagenomic sequences were deposited in EBI under accession PRJEB14154.

Results and discussion

hgcAB genes

PCR amplifications targeting the *hgcAB* genes produced visible bands in 8 out of 193 samples from the Arctic Ocean,

from which five nucleic acid sequences were obtained by Sanger sequencing (565 ± 238 bp). However, no evidence for the presence of *hgcAB* was found from the resulting sequences. Amplicon sequences did not match any sequences in Genbank's nonredundant (nt) database using BLASTn with default parameters, but when translated into amino acid sequences (BLASTx) some partial matches were observed in the nonredundant "nr" database with query coverages of 11–15%. Partial matches included nitrogenase reductase (e-value = 4×10^{-4}), nonribosomal peptide synthetase (e-value = 3×10^{-7}), and methyl-coenzyme M reductase (e-value = 5×10^{-5}) found in methanogenic archaea. Translated amplicon sequences from three samples were found to contain a 7-residue motif conserved in HgcA (Parks et al. 2013), but no other homology to HgcA or HgcA-like proteins was evident (Fig. 2). These amplicon sequences were found near the center of the Arctic Ocean in the transpolar drift (TPD; Sta. 30, 24 m depth, n = 2) and in a benthic nepheloid layer (BNL; Sta. 26, 2901 m depth, n = 1). The TPD is a surface current that carries sea ice, suspended shelf material, and river water from the Laptev and East Siberian Seas to the central Arctic Ocean before reaching the Fram Strait (Rudels et al. 2001). Discovery of amplicon sequences with part of the conserved motif of HgcA is intriguing because most known methylating organisms with the *hgcAB* gene cluster are found in the benthos (Gilmour et al. 2013; Podar et al. 2015). Clade-specific qPCR did not amplify *hgcA* in gDNA samples from the Arctic Ocean. The relative limit of detection (50–680 copies of *hgcA*) represents ~ 0.002 ng of DNA from positive control organisms; therefore, in order to amplify *hgcA*, more than 0.2% of gDNA tested would have to be *hgcA* positive.

Several metagenomic reads matched *hgcB* when using HMMs, but because the ferredoxin-encoding domain is widespread in prokaryotic genomes, these hits do not confirm the presence of *hgcAB*. No HMM hits to *hgcA* were observed from the Arctic Ocean (Sta. 26, 30, and 60). However, sequences from CdhD proteins (TIM barrel of acetyl-CoA synthase delta subunit, IPR016041), paralogous to HgcA, were found at Sta. 60 and 30.

hgcA-like genes

HgcA-like sequences from the equatorial North Pacific (previously reported by Podar et al. 2015) were compared with HgcA sequences from known methylators and HgcA-like peptides from Antarctic sea ice (Gionfriddo et al. 2016) (Fig. 2). Sequences from the Arctic Ocean (*hgcA*-PCR amplicons and CdhD sequences; this study) showed poor alignment. The conserved motif of the cobalamin-binding domain was identical in sequences from the equatorial North Pacific and Antarctic sea ice (Gionfriddo et al. 2016). HgcA-like sequences from these marine environments are closely related to HgcA-like protein encoded by *Nitrospina*, the most common nitrite-oxidizing bacterium in the ocean. At this time, *Nitrospina* has not been tested for the ability to produce MMHg; however, the amino acid substitutions in *hgcA-like* genes are not predicted to impede Hg methylation (Podar et al. 2015; Smith et al. 2015).

MMHg distribution and Hg-cycling genes

The oxygen minimum zone (OMZ) of the equatorial North Pacific Ocean (MetZyme expedition) is one of few locations in the marine water column where *hgcA-like* genes have been found (Podar et al. 2015; Gionfriddo et al. 2016). The MetZyme transects include one station (Sta. 3, 8°N 156°W) where both mercury speciation (Munson et al. 2015) and metagenomic (Santoro et al. 2017) data are available (Fig. 3). Surprisingly, we discovered *merB* and *merR*, in addition to previously described *hgcA*-like sequences, in the OMZ at this station. The *mer* operon is only known to be active at elevated (nanomolar range) Hg concentrations (Schaefer et al. 2004; Kritee et al. 2007, 2009); however, *mer* genes have previously been found in biomass from the coast of Canada (Poulain et al. 2007) at Hg concentrations similar to the open-ocean (picomolar range). Munson et al. (2018) conducted incubation

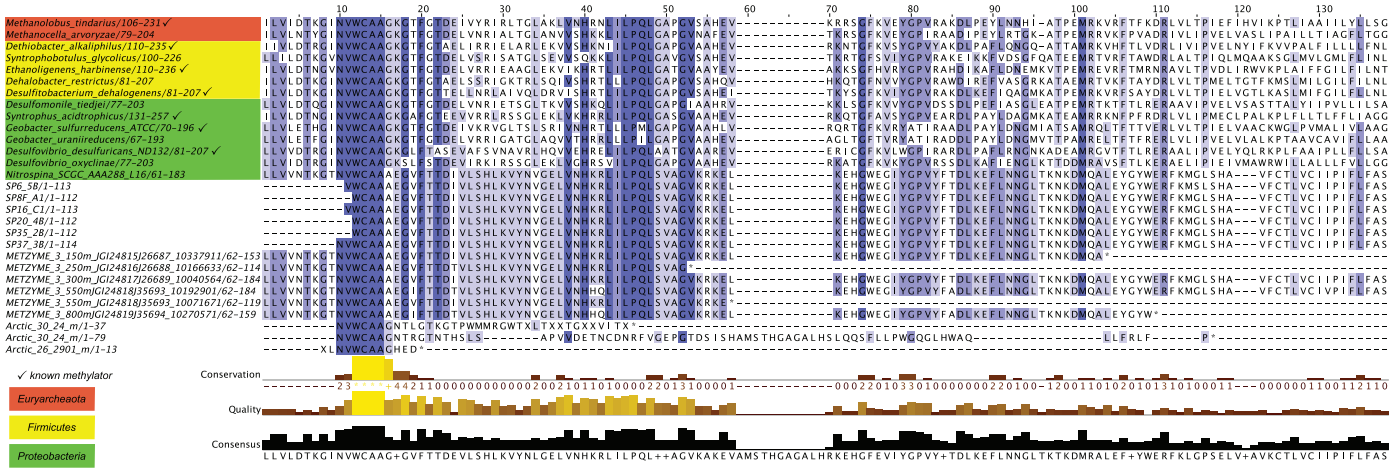

Fig. 2. Sequence comparison plot for *hgcA* from known methylators (Parks et al. 2013) and *hgcA*-like genes from Antarctic Sea ice ("SP"; Gionfriddo et al. 2015), equatorial North Pacific seawater ("METZYME"; Santoro et al. 2017), and Arctic Ocean seawater ("Arctic"; this study).

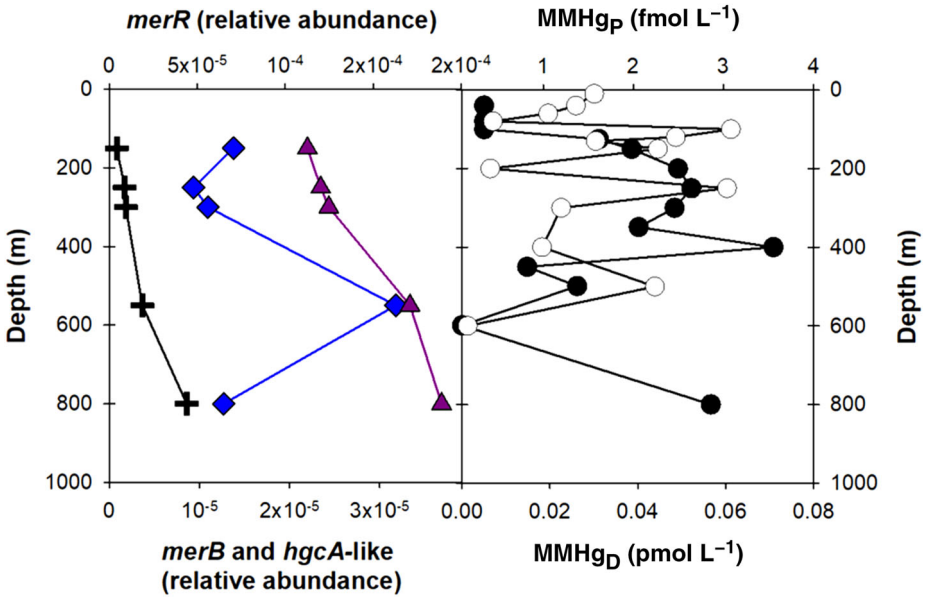

Fig. 3. Relative abundance of mercury cycling genes and MMHg concentrations in the equatorial North Pacific Ocean (8°N, 156°W). The left panel shows the relative abundances of *hgcA*-like (cross), *merB* (diamond), and *merR* (triangle) genes, and the right panel shows particulate MMHg (MMHg$_P$; white circles) and dissolved MMHg (MMHg$_D$; black circles) concentrations.

experiments with isotopically enriched Hg isotopes and measured net demethylation in the OMZ at Sta. 3 (200 m, 15 μm kg^{-1} O_2). Expression of Hg cycling genes was not measured during these incubations; however, we found the ambient relative abundance of *merB* and *merR* to exceed that of *hgcA-like* genes (Fig. 3), consistent with net demethylation of MMHg in this region of the water column.

Genes from the *mer* operon and *hgcA*-like paralogs (*cdhD*) were found in Arctic Ocean metagenomes in the Makarov Basin and at the Chukchi shelf (Figs. 4–5). Stations 26 and 30 in the Makarov Basin were ice-covered and the underlying water column was divided into the polar mixed layer (0–51 m), the halocline (> 51–100 m), Atlantic Water (> 100–400 m), and Canada basin deep water (CBDW; Rudels 2001; Supporting Information Figs. S1, S2). The upper water column (< 400 m) at Sta. 26 had relatively low dissolved and particulate MMHg, and *merR* but no *merB* was present (Fig. 4A). In the halocline, particulate MMHg and Hg^0 (Supporting Information Fig. S1) increased slightly and *merR* abundance decreased. The halocline receives brine rejected during sea ice formation and this layer has distinct geochemical characteristics (Anderson et al. 2013) that can impact Hg chemistry and microbial communities.

The relative abundance of *arsR* at Sta. 30 was similar to *merR* at Sta. 26 (both activator/repressors of the *mer* operon), and *merB* and *cdhD* genes were found in the upper water column (Fig. 4B). Unlike Sta. 26, the upper water column at Sta. 30 lies within the TPD. Kipp et al. (2018) used a short-lived radium isotope, ^{228}Ra, to monitor sediment input from the TPD along the Arctic transect. ^{228}Ra was detected in the upper 400 m of the water column at Sta. 30 (greatest concentrations < 100 m) and transport estimates suggest a 6–12 month transport time from the Siberian shelf (Kipp et al. 2018). In the upper water column where ^{228}Ra was detected, dissolved MMHg concentrations were greater (0.096 ± 0.078 pmol L^{-1}, n = 10) than water from the same depth at Sta. 26 (0.046 ± 0.026 pmol L^{-1}, n = 8), while particulate MMHg concentrations were similar. At the Chukchi shelf, MMHg increased near the benthos (~ 5 m from bottom) at Sta. 6 and 66 (0.04 pmol L^{-1} dissolved MMHg, n = 1; 1.4 ± 0.3 fmol L^{-1} particulate MMHg, n = 2; Supporting Information Fig. S4). If we assume that concentrations of MMHg over the Siberian Shelf are similar to the Chukchi shelf, and use a demethylation rate determined for polar marine waters (0.36 ± 0.09 d^{-1}, Lehnherr et al. 2011), then all shelf derived MMHg should be demethylated during the 6–12 month transport time. This suggests that elevated MMHg in the upper water column at Sta. 30 is the product of in situ methylation.

Despite greater concentrations of total Hg in overlying sea ice at Sta. 30 (2.2 ± 1.4 pmol L^{-1}, n = 24, DiMento et al. 2018) compared to the upper water column (< 400 m; 0.70 ± 0.22 pmol L^{-1}, n = 9), the average abundance of *merR* was an order of magnitude greater and *merB* three orders of magnitude greater in seawater compared to ice (this study). Furthermore, no *cdhD* genes were found in overlying sea ice. This indicates the TPD, rather than overlying sea ice, as a source of Hg cycling genes to the central Arctic Ocean.

In CBDW, the relative abundance of *merB*, *merR*, and *arsR*, and concentrations of dissolved and particulate MMHg remained fairly constant. An increase in the relative abundance of *merB* and *merR* can be seen in a BNL ~ 2800 m at Sta. 26 (Fig. 4A), and an increase in the relative abundance of

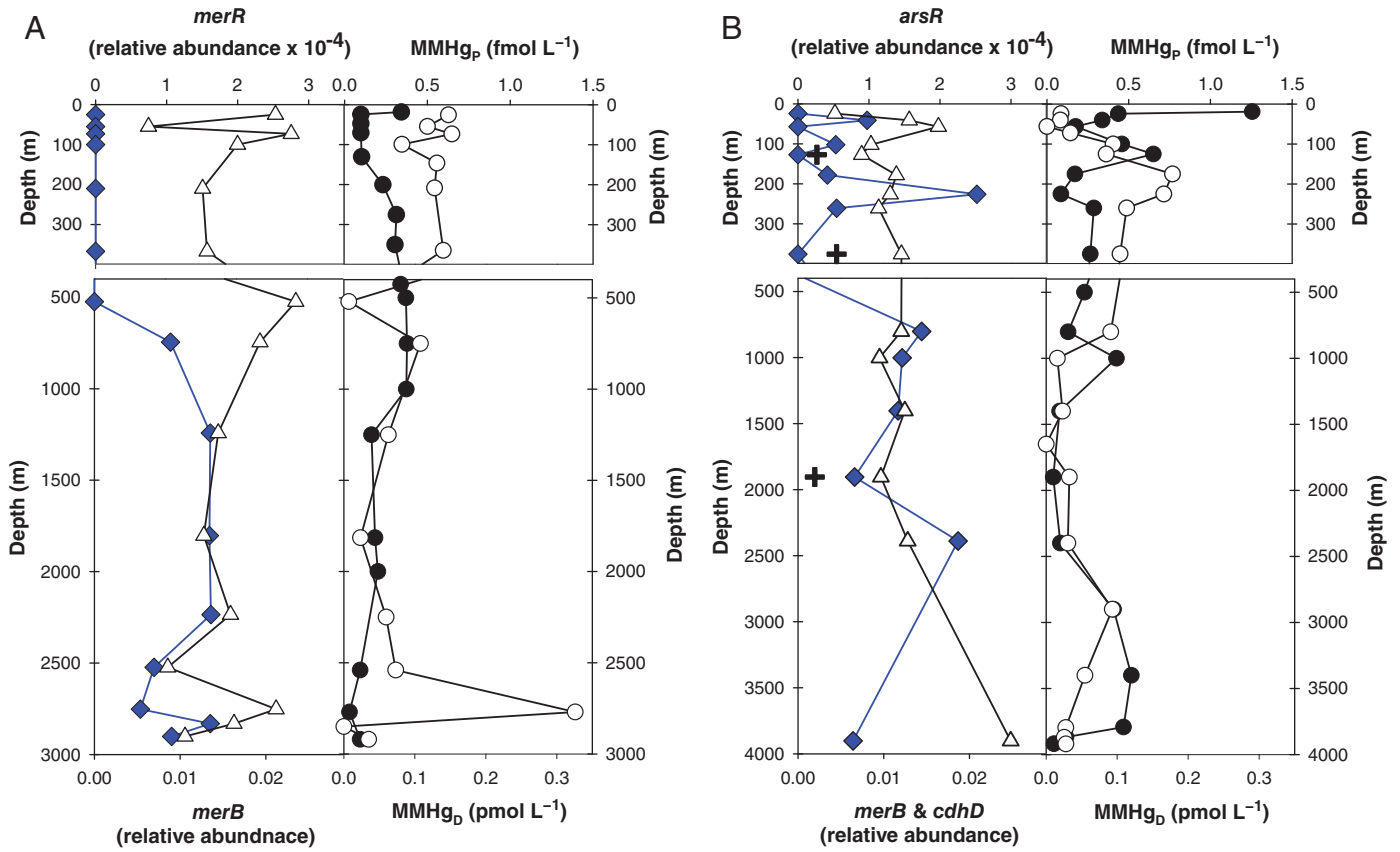

Fig. 4. Relative abundance of mercury cycling genes and MMHg concentrations in the central Arctic Ocean at Sta. 26 (**A**) and Sta. 30 (**B**). The left panels show relative abundances of *merB* (diamond), *merR* or *arsR* (triangle), and *cdhD* (cross) genes, and the right panels show particulate MMHg ($MMHg_P$; white circles) and dissolved MMHg ($MMHg_D$; black circles) concentrations.

arsR was observed in a BNL ~ 3800 m at Sta. 30 (Fig. 4B). Scavenging in the BNL appeared to control dissolved and particulate MMHg concentrations near the benthos at Sta. 26 (Fig. 4A).

Mercury-cycling genes and MMHg concentrations appear to be influenced by the benthos near the Chukchi shelf (Sta. 60, Fig. 5). Sediment-derived materials are transported off the Chukchi shelf via the eastward flowing shelfbreak jet and the westward flowing Chukchi slope current (Corlett and Pickart 2017; Kipp et al. 2019). Shelf-influenced water delivered by these currents is found between 26 and 180 m (σ = 24–27; Kipp et al. 2019) and here we observed an increase in the relative abundance of *arsR* and *merB* and a slight increase in dissolved and particulate MMHg concentrations (Fig. 5). Below 415 m, there was a large BNL where *arsR*, *merB*, and *cdhD* genes were found and particulate MMHg increased and dissolved MMHg was likely scavenged (Fig. 5).

The source of MMHg and Hg-cycling genes at Sta. 60 could be isopycnal transport of resuspended shelf and slope material, or in situ production of MMHg and increased microbial abundance stimulated by the introduction of cells and metabolites from the benthos. Production and efflux of MMHg is considered a significant source of MMHg to coastal waters in the northwest Atlantic Ocean (Hammerschmidt et al. 2004, 2006; Hollweg et al. 2010) and Hg-cycling genes (*hgcA* and *mer* genes) have been detected in marine sediments at lower latitudes (Reyes et al. 1999; Podar et al. 2015; Zheng et al. 2018), though similar studies are lacking in the Chukchi Sea. Using the same shelf transport calculation described above, we estimate that shelf-derived MMHg delivered via the Chukchi slope current (20 cm s^{-1} speed via the Barrow Canyon; Corlett and Pickart 2017) represents 2–3% of average particulate and dissolved MMHg concentrations at Sta. 60 between shelf-influenced density isopycnals (σ = 24–27). Shelf-derived MMHg from the shelfbreak jet would be negligible due to slower speed (8 cm s^{-1}) and greater distance from its origin at the Herald Canyon (Corlett and Pickart 2017); however, eddies stemming from the shelfbreak jet could decrease transport time (Kipp et al. 2019). Maxima of MMHg at Sta. 60, therefore, are more likely the product of in situ Hg methylation. This is consistent with studies in the Beaufort Sea and the central and western Arctic Ocean where the shelf-derived apparent oxygen utilization did not correlate with MMHg concentrations and estimated shelf inputs were negligible (Wang et al. 2012; Heimbürger et al. 2015; Agather et al. In press). Uchimiya et al. (2016) observed an increase in bacterial

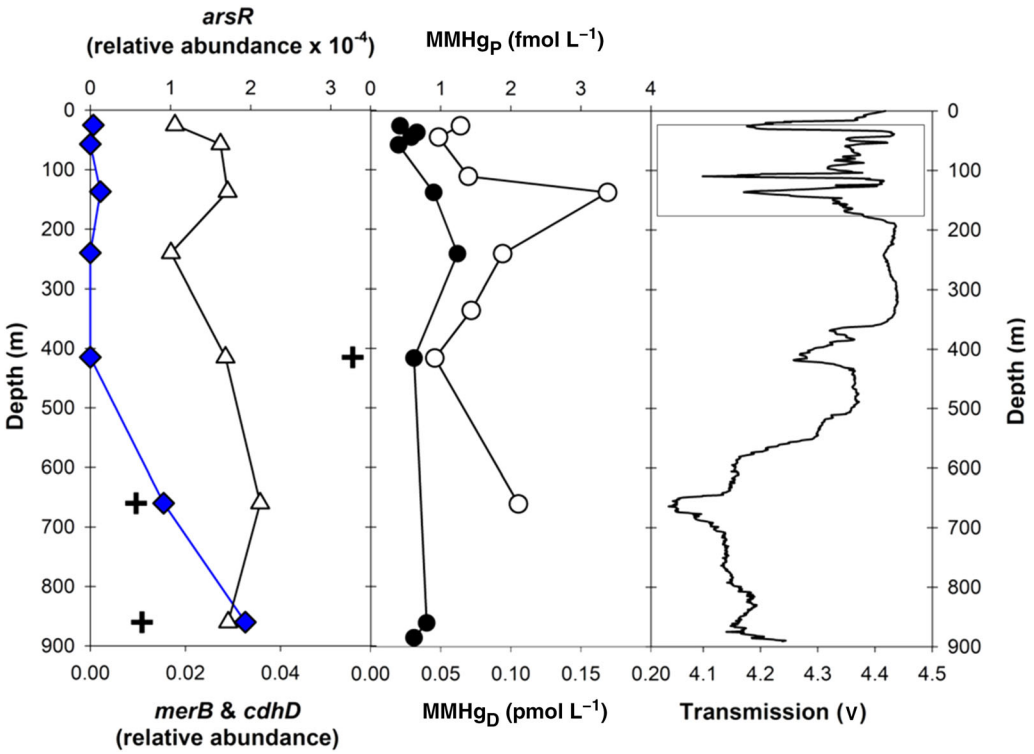

Fig. 5. Relative abundance of mercury-cycling genes and MMHg concentrations at the Chukchi shelf (Sta. 60). The left panel shows the relative abundances of *merB* (diamond), *arsR* (triangle), and *cdhD* (cross) genes, the middle panels shows particulate MMHg ($MMHg_P$; white circles) and dissolved MMHg ($MMHg_D$; black circles) concentrations, and the right panel shows transmission with a box outlining shelf-influenced density isopycnals (σ = 24–27).

abundance over the Chukchi shelf associated with wind-driven sediment resuspension and it is possible that similar processes caused an increase in the relative abundance of Hg-cycling genes in shelf-influenced waters and the BNL.

Taxa related to known methylators

Bacteria and *Archaea* related to known Hg methylators were identified by taxonomic classification in the Arctic and equatorial North Pacific Ocean metagenomes. *Nitrospina*, the nitrite-oxidizing bacterium with an *hgcA*-like gene (Gionfriddo et al. 2016), was found in the OMZ of the equatorial North Pacific, at Arctic Ocean Sta. 30 in the TPD (Fig. 6), and in CBDW (Sta. 30 at 2961 m depth, Sta. 26 at 2235 m depth). The Arctic Ocean metagenome also contained sequences from *Desulfobacteraceae*, a family of sulfate-reducing bacteria that includes six species of known methylators, one with the *hgcAB* gene cluster (*Desulfococcus multivorans*, Gilmour et al. 2013); these sequences were found in sediment-influenced waters in the BNL at Sta. 60 near the Chukchi shelf and within the TPD at Sta. 30 (Fig. 6). Organisms from the *Methanomassiliicoccus* genus of methanogens were identified in the equatorial North Pacific metagenome; this genus includes *Methanomassiliicoccus luminyensis*, a species of proven Hg-methylations with the *hgcAB* gene cluster (Gilmour et al. 2013; Gilmour et al. 2018; Fig. 6).

Taxa and functional gene correlations with Hg concentrations

To expand our search for other microorganisms that may influence Hg chemistry, we looked for correlations between Hg species concentrations and the relative abundance of functional genes and prokaryotic taxa in the Arctic Ocean metagenome (Supporting Information Tables S2–S5). The same was not attempted with the equatorial North Pacific metagenome due to small sample size (n = 5 depths). Various functional genes correlated with dissolved and particulate MMHg concentrations at Sta. 26, 30, and 60 (Supporting Information Tables S4, S5). At Sta. 30, two families of methyltransferases that catalyze the methylation of corrinoid proteins (trimethylamine methyltransferase, tetrapyrrole methylase) correlated with dissolved MMHg concentrations (r = 0.73, p = 0.002 and r = 0.71, p = 0.003, respectively). Tetrapyrrole methylase is involved in the biosynthesis of cobalamin (Raux et al. 2000) and trimethylamine methyltransferase is involved in methanogenesis (Paul et al. 2000). Methanogens in culture have recently been shown to produce MMHg at a rate similar to sulfate- and iron-reducing *Deltaproteobacteria* (Gilmour et al. 2018). Proteins associated with the coenzyme-A pathway correlated with both dissolved (Sta. 26, r = 0.62, p = 0.015, Sta. 60, r = 0.90, p = 0.006) and particulate (Sta. 26, r = 0.75, p = 0.001) MMHg. These correlations are consistent with previously described pathways of Hg methylation (Choi et al. 1994*a*,*b*; Parks et al. 2013).

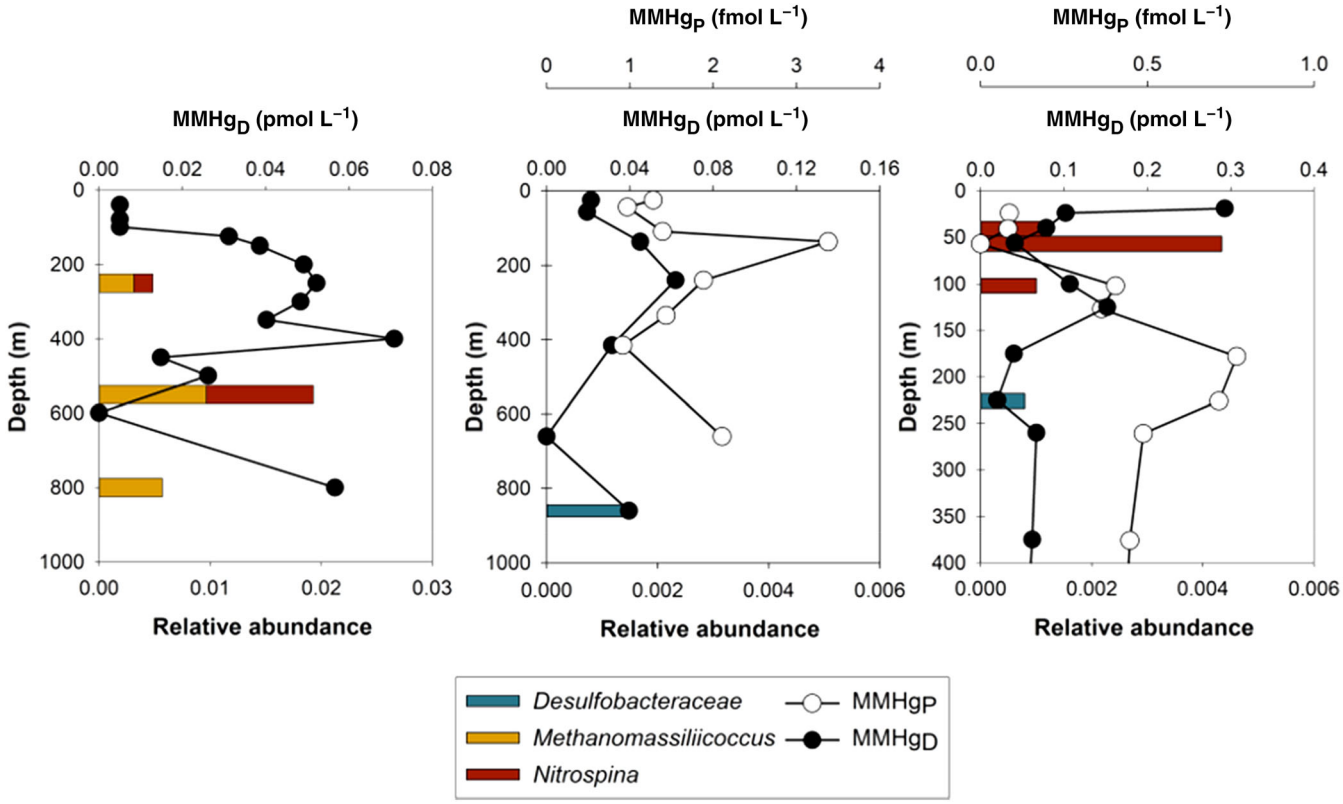

Fig. 6. Dissolved ($MMHg_D$) and particulate ($MMHg_P$) monomethylmercury concentrations in the upper water column and relative abundances of taxa related to known mercury methylators in the equatorial North Pacific Sta. 3 (left), Chukchi shelf Sta. 60 (middle), and central Arctic Ocean Sta. 30 (right).

Dissolved and particulate MMHg at Sta. 30 correlated with enzymes that require a divalent metal cation (e.g., Zn^{2+}) for activation (r = 0.71–0.76, $p < 0.003$; Supporting Information Tables S4, S5). Substitution of Hg^{2+} for divalent metal cations such as Zn^{2+} and Cd^{2+} has been shown in some metalloenzymes (Bertini and Luchinat 1994), and could serve as a gateway for inorganic Hg into a biochemical pathway that ultimately leads to the production of MMHg. Functional genes with a 4Fe-4S binding domain correlated with dissolved MMHg at Sta. 26, 30, and 60 (r = 0.66–0.85, $p < 0.02$; Supporting Information Table S4). Iron-sulfur binding domains may serve as a reductase, fulfilling the role of HgcB in corrinoid ring reduction, or the four cysteine residues thought to bind 4Fe-4S proteins (den Hengst and Buttner 2008) may serve as thiolate ligands for intracellular Hg.

Conclusions

Observational and rate measurement studies in the marine water column support the hypothesis that microorganisms contribute to Hg-methylation in the ocean. However, the only microbial genes presently known to control Hg-methylation (*hgcAB*) are absent from seawater. Our results suggest that *hgcA* genes are not present in the Arctic Ocean, or that *hgcA* was present at a low abundance not captured by our analytical methods. If the latter is true, our taxonomic analysis revealed the most likely candidate for possessing the *hgcAB* cluster to be from the *Desulfobacteraceae* family of sulfate-reducing bacteria, found in sediment-influence water in the Arctic Ocean. Other functional genes, such as methyltransferases and proteins associated with the coenzyme-A pathway, could play a role in Hg-methylation in the ocean.

The role of *hgcA*-like genes in Hg-methylation has not been tested, but the nucleic acid substitutions found in *hgcA*-like genes are not predicted to impede Hg methylation (Podar et al. 2015; Smith et al. 2015). The *Nitrospina* genus, which includes species possessing *hgcA*-like genes, was found in the equatorial North Pacific and in the central Arctic Ocean in the TPD. Sequence similarity between *hgcA*-like genes in the equatorial North Pacific and Antarctic sea ice suggests that *Nitrospina*, if proven to methylate Hg, has a far-reaching influence on MMHg distribution in the ocean.

Genes from the *mer* operon were present in seawater from the equatorial North Pacific and Arctic oceans. The absence of *merA* in the Arctic water column is surprising with the presence of *merR* and both inner membrane and periplasmic Hg(II) transporter genes. It is possible that a homolog of *merA* was present in these samples that was not captured by our analysis. Future studies are needed to determine the expression of *mer* genes at low-Hg concentrations and the importance of the *mer* operon to demethylation of MMHg in the ocean.

Our analysis of Hg cycling genes in the Arctic and equatorial North Pacific oceans suggests the absence or low abundance of

hgcA genes, the presence of *mer* genes, and highlights the need for coupled gene expression and Hg-methylation experiments to understand genomic controls on net production of MMHg in the ocean.

References

Agather, A. M., K. L. Bowman, C. H. Lamborg, and C. R. Hammerschmidt. 2019. Distribution of mercury species in the western Arctic Ocean (U.S. GEOTRACES GN01). Mar. Chem. **216**. doi:10.1016/j.marchem.2019.103686.

Anderson, L. G., P. S. Andersson, G. Björk, E. P. Jones, S. Jutterström, and E. Wåhlström. 2013. Source and formation of the upper halocline of the Arctic Ocean. J. Geophys. Res. Oceans **118**: 410–421. doi:10.1029/2012JC008291.

Barkay, T., S. M. Miller, and A. O. Summers. 2003. Bacterial mercury resistance from atoms to ecosystems. FEMS Microbiol. Rev. **27**: 355–384. doi:10.1016/S0168-6445(03)00046-9.

Bertini, I., and C. Luchinat. 1994. The reaction pathways of zinc enzymes and related biological catalysts, p. 37–106. *In* I. Bertini, H. B. Gray, S. J. Lippard, and J. S. Valentine [eds.], Bioinorganic chemistry. Univ. Science Books.

Bianchi, D., T. S. Weber, R. Kiko, and C. Deutsch. 2018. Global niche of marine anaerobic metabolisms expanded by particle microenvironments. Nat. Geosci. **11**: 263–268. doi:10.1038/s41561-018-0081-0.

Bishop, J. K. B., P. J. Lam, and T. J. Wood. 2012. Getting good particles: Accurate sampling of particles by large volume in-situ filtration. Limnol. Oceanogr.: Methods **10**: 681–710. doi:10.4319/lom.2012.10.681.

Bowman, K. L., and C. R. Hammerschmidt. 2011. Extraction of monomethylmercury from seawater for low-femtomolar determination. Limnol. Oceanogr.: Methods **9**: 121–128. doi:10.4319/lom.2011.9.121.

Bowman, K. L., C. R. Hammerschmidt, C. H. Lamborg, and G. Swarr. 2015. Mercury in the North Atlantic Ocean: The U.S. GEOTRACES zonal and meridional sections. Deep-Sea Res. Part II Top. Stud. Oceanogr. **116**: 251–261. doi:10.1016/j.dsr2.2014.07.004.

Bowman, K. L., C. R. Hammerschmidt, C. H. Lamborg, G. J. Swarr, and A. M. Agather. 2016. Distribution of mercury species across a zonal section of the eastern tropical South Pacific Ocean (U.S. GEOTRACES GP16). Mar. Chem. **186**: 156–166. doi:10.1016/j.marchem.2016.09.005.

Boyd, E. S., and T. Barkay. 2012. The mercury resistance operon: From an origin in a geothermal environment to an efficient detoxification machine. Front. Microbiol. **3**: 349. doi:10.3389/fmicb.2012.00349.

Brown, N. L., J. V. Stoyanov, S. P. Kidd, and J. L. Hobman. 2003. The MerR family of transcriptional regulators. FEMS Microbiol. Rev. **27**: 145–163. doi:10.1016/S0168-6445(03)00051-2.

Busenlehner, L. S., M. A. Pennella, and D. P. Giedroc. 2003. The SmtB/ArsR family of metalloregulatory transcriptional repressors: Structural insights into prokaryotic metal resistance. FEMS Microbiol. Rev. **27**: 131–143. doi:10.1016/S0168-6445(03)00054-8.

Choi, S. C., T. Chase, and R. Bartha Jr. 1994*a*. Metabolic pathways leading to mercury methylation in *Desulfovibrio desulfuricans* LS. Appl. Environ. Microbiol. **60**: 4072–4077.

Choi, S. C., T. Chase, and R. Bartha Jr. 1994*b*. Enzymatic catalysis of mercury methylation by *Desulfovibrio desulfuricans* LS. Appl. Environ. Microbiol. **60**: 1342–1346.

Christensen, G. A., and others. 2016. Development and validation of broad-range qualitative and clade-specific quantitative molecular probes for assessing mercury methylation in the environment. Appl. Environ. Microbiol. **82**: 6068–6078. doi:10.1128/AEM.01271-16.

Corlett, W. B., and R. S. Pickart. 2017. The Chukchi slope current. Prog. Oceanogr. **153**: 50–65. doi:10.1016/j.pocean.2017.04.005.

Cossa, D., and others. 2011. Mercury in the Southern Ocean. Geochim. Cosmochim. Acta **75**: 4037–4052. Biogeosciences 15: 2309–2323. doi:10.1016/j.gca.2011.05.001.

Cossa, D., and others. 2018. Mercury distribution and transport in the North Atlantic Ocean along the GEOTRACES-GA01 transect. Mar. Chem. **198**: 64–69. doi:10.1016/j.marchem.2017.11.006.

Cutter, G. A., and K. W. Bruland. 2012. Rapid and noncontaminating sampling system for trace elements in global ocean surveys. Limnol. Oceanogr.: Methods **10**: 425–436. doi:10.4319/lom.2012.10.425.

Debes, F., P. Weihe, and P. Grandjean. 2016. Cognitive deficits at age 22 years associated with prenatal exposure to methylmercury. Cortex **74**: 358–369. doi:10.1016/j.cortex.2015.05.017.

den Hengst, C. D., and M. J. Buttner. 2008. Redox control in actinobacteria. Biochim. Biophys. Acta **1780**: 1201–1216. doi:10.1016/j.bbagen.2008.01.008.

DiMento, B. P., R. P. Mason, S. Brooks, and C. Moore. 2018. The impact of sea ice on the air-sea exchange of mercury in the Arctic Ocean. Deep-Sea Res. Part I Oceanogr. Res. Pap. **144**: 28–38. doi:10.1016/j.dsr.2018.12.001.

Gilmour, C. C., and others. 2013. Mercury methylation by novel microorganisms from new environments. Environ. Sci. Technol. **47**: 11810–11820. doi:10.1021/es403075t.

Gilmour, C. C., A. L. Bullock, A. McBurney, M. Podar, and D. A. Elias. 2018. Robust mercury methylation across diverse methanogenic archaea. mBio **9**: e02403–e02417. doi:10.1128/mBio.02403-17.

Gionfriddo, C. M., and others. 2016. Microbial mercury methylation in Antarctic Sea ice. Nat. Microbiol. **1**: 16127. doi:10.1038/NMICROBIOL.2016.127.

Hammerschmidt, C. R., W. F. Fitzgerald, C. H. Lamborg, P. H. Balcom, and P. T. Visscher. 2004. Biogeochemistry of methylmercury in sediments of Long Island Sound. Mar. Chem. **90**: 31–52. doi:10.1016/j.marchem.2004.02.024.

Hammerschmidt, C. R., and W. F. Fitzgerald. 2006. Methylmercury cycling in sediments on the continental shelf of southern New England. Geochim. Cosmochim. Acta **70**: 918–930. doi:10.1016/j.gca.2005.10.020.

Heimbürger, L. E., and others. 2015. Shallow methylmercury production in the marginal sea ice zone of the central Arctic Ocean. Sci. Rep. **5**: 10318. doi:10.1038/srep10318.

Hollweg, T. A., C. C. Gilmour, and R. P. Mason. 2010. Mercury and methylmercury cycling in sediments of the mid-Atlantic continental shelf and slope. Limnol. Oceanogr. **55**: 2703–2722. doi:10.4319/lo.2010.55.6.2703.

Kipp, L. E., M. A. Charette, W. S. Moore, P. B. Henderson, and I. G. Rigor. 2018. Increased fluxes of shelf-derived materials to the central Arctic Ocean. Sci. Adv. **4**: eaao1302. doi:10.1126/sciadv.aao1302.

Kipp, L. E., D. C. Kadko, R. S. Pickart, P. B. Henderson, W. S. Moore, and M. A. Charette. 2019. Shelf-basin interactions and water mass residence times in the western Arctic Ocean: Insights provided by radium isotopes. J. Geophys. Res. **124**: 3279–3297. doi:10.1029/2019JC014988.

Kritee, K., J. D. Blum, M. W. Johnson, B. A. Bergquist, and T. Barkay. 2007. Mercury stable isotope fractionation during reduction of Hg(II) to Hg(0) by mercury resistant microorganisms. Environ. Sci. Technol. **41**: 1889–1895. doi:10.1021/es062019t.

Kritee, K., T. Barkay, and J. Blum. 2009. Mass dependent stable isotope fractionation of mercury during *mer* mediated microbial degradation of monomethylmercury. Geochim. Cosmochim. Acta **73**: 1285–1296. doi:10.1016/j.gca.2008.11.038.

Lam, P. J., B. S. Twining, C. Jeandel, A. Roychoudhury, J. A. Resing, P. H. Santschi, and R. F. Anderson. 2015. Methods for analyzing the concentration and speciation of major and trace elements in marine particles. Prog. Oceanogr. **133**: 32–42. doi:10.1016/j.pocean.2015.01.005.

Lamborg, C. H., and others. 2014. A global ocean inventory of anthropogenic mercury based on water column measurements. Nature **512**: 65–68. doi:10.1038/nature13563.

Lehnherr, I., V. L. St Louis, H. Hintelmann, and J. L. Kirk. 2011. Methylation of inorganic mercury in polar marine waters. Nat. Geosci. **4**: 298–302. doi:10.1038/ngeo1134.

Madigan, D. L., and others. 2018. Mercury stable isotopes reveal influence of foraging depth on mercury concentrations and growth in Pacific bluefin tuna. Environ. Sci. Technol. **52**: 6256–6264. doi:10.1021/acs.est.7b06429.

Mason, R. P., and W. F. Fitzgerald. 1993. The distribution and biogeochemical cycling of mercury in the equatorial Pacific Ocean. Deep-Sea Res. Part I Oceanogr. Res. Pap. **40**: 1897–1924. doi:10.1016/0967-0637(93)90037-4.

Mason, R. P., K. R. Rolfhus, and W. F. Fitzgerald. 1995. Methylated and elemental mercury cycling in surface and deep ocean waters of the North Atlantic. Water Air Soil Pollut. **80**: 665–677. doi:10.1007/BF01189719.

Mitchell, A. L., and others. 2018. EBI metagenomics in 2017: Enriching the analysis of microbial communities, from sequence reads to assemblies. Nucleic Acids Res. **46**: D726–D735. doi:10.1093/nar/gkx967.

Monperrus, M., E. Tessier, D. Amouroux, A. Leynaert, P. Huonnic, and O. F. X. Donard. 2007. Mercury methylation, demethylation and reduction rates in coastal and marine surface waters of the Mediterranean Sea. Mar. Chem. **107**: 49–63. doi:10.1016/j.marchem.2007.01.018.

Munson, K. M., D. Babi, and C. H. Lamborg. 2014. Determination of monomethylmercury from seawater with ascorbic acid-assisted direct ethylation. Limnol. Oceanogr.: Methods **12**: 1–9. doi:10.4319/lom.2014.12.1.

Munson, K. M., C. H. Lamborg, G. J. Swarr, and M. A. Saito. 2015. Mercury species concentrations and fluxes in the Central Tropical Pacific Ocean. Global Biogeochem. Cycles **29**: 656–676. doi:10.1002/2015GB005120.

Munson, K. M., C. H. Lamborg, R. M. Boiteau, and M. A. Saito. 2018. Role of non-cellular methylation in mercury dynamics of oligotrophic waters. Biogeosciences **15**: 6451–6460. doi:10.5194/bg-2018-173.

Ortiz, V. L., R. P. Mason, and J. E. Ward. 2015. An examination of the factors influencing mercury and methylmercury particulate distributions, methylation and demethylation rates in laboratory-generated marine snow. Mar. Chem. **177**: 753–762. doi:10.1016/j.marchem.2015.07.006.

Parks, J. M., and others. 2013. The genetic basis for bacterial mercury methylation. Science **339**: 1332–1335. doi:10.1126/science.1230667.

Paul, L., D. J. Ferguson, and J. A. Krzycki. 2000. The trimethylamine methyltransferase gene and multiple dimethylamine methyltransferase genes of *Methanosarcina barkeri* contain in-frame and read-through amber codons. J. Bacteriol. **182**: 2520–2529. doi:10.1128/JB.182.9.2520-2529.2000.

Podar, M., and others. 2015. Global prevalence and distribution of genes and microorganisms involved in mercury methylation. Sci. Adv. **1**: e1500675. doi:10.1126/sciadv.1500675.

Poulain, A. J., S. M. Ní Chadhain, P. A. Ariya, M. Amyot, E. Garcia, P. G. C. Campbell, G. J. Zylstra, and T. Barkay. 2007. Potential for mercury reduction by microbes in the high Arctic. Appl. Environ. Microbiol. **73**: 2230–2238. doi:10.1128/AEM.02701-06.

Raux, E., H. L. Schubert, and M. J. Warren. 2000. Biosynthesis of cobalamin (vitamin B12): A bacterial conundrum. Cell. Mol. Life Sci. **57**: 1880–1893. doi:10.1007/PL00000670.

Reyes, N. S., M. E. Frischer, and P. A. Sobecky. 1999. Characterization of mercury resistance mechanisms in marine sediment microbial communtities. FEMS Microbiol. Ecol. **30**: 273–284. doi:10.1111/j.1574-6941.1999.tb00655.x.

Rudels, B. 2001. Arctic Basin circulation, p. 177–187. *In* J. H. Steele, S. A. Thorpe, and K. K. Turekian [eds.], Encyclopedia of ocean sciences. Elsevier Science.

Saito, M. A., M. R. McIlvin, D. Moran, T. J. Goepfert, G. R. DiTullio, A. F. Post, and C. H. Lamborg. 2014. Multiple nutrient stresses at intersecting Pacific Ocean biomes detected by protein biomarkers. Science **345**: 1173–1177. doi:10.1126/science.1256450.

Santoro, A. E., M. A. Saito, T. J. Goepfert, C. H. Lamborg, C. L. Dupont, and G. R. DiTullio. 2017. Thaumarchael ecotype distributions across the equatorial Pacific Ocean and their

potential roles in nitrification and sinking flux attenuation. Limnol. Oceanogr. **62**: 1984–2003. doi:10.1002/lno.10547.

Schaefer, J. K., J. Yagi, J. R. Reinfelder, T. Cardona, K. M. Ellickson, S. Tel-Or, and T. Barkay. 2004. Role of the bacterial organomercury lyase (MerB) in controlling methylmercury accumulation in mercury-contaminated natural waters. Environ. Sci. Technol. **38**: 4304–4311. doi:10.1021/es049895w.

Schartup, A. T., A. Qureshi, C. Dassuncao, C. P. Thackray, G. Harding, and E. M. Sunderland. 2018. Methylmercury uptake and trophic transfer by marine plankton. Environ. Sci. Technol. **52**: 654–662. doi:10.1021/acs.est.7b03821.

Smith, S. D., and others. 2015. Site-directed mutagenesis of HgcA and HgcB reveals amino acid residues important for mercury methylation. Appl. Environ. Microbiol. **81**: 3205–3217. doi:10.1128/AEM.00217-15.

Stoddard, S. F., B. J. Smith, R. Hein, B. R. K. Roller, and T. M. Schmidt. 2015. rrnDB: Improved tools for interpreting rRNA gene abundance in bacteria and archaea and a new foundation for future development. Nucleic Acids Res. **43**: D593–D598. doi:10.1093/nar/gku1201.

Sunderland, E. M., D. P. Krabbenhoft, J. W. Moreau, S. A. Strode, and W. M. Landing. 2009. Mercury sources, distribution, and bioavailability in the North Pacific Ocean: Insights from data and models. Global Biogeochem. Cycles **23**: GB2010. doi:10.1029/2008GB003425.

Sunderland, E. M., M. Li, and K. Bullard. 2018. Decadal changes in edible supply of seafood and methylmercury exposure in the United States. Environ. Health Perspect. **126**: EHP2644. doi:10.1289/EHP2644.

Tseng, C.-M., C. R. Hammerschmidt, and W. F. Fitzgerald. 2004. Determination of methylmercury in environmental matrixes by on-line flow injection and atomic fluorescence spectrometry. Anal. Chem. **76**: 7131–7136. doi:10.1021/ac049118e.

Turner, S., K. M. Pryer, V. P. W. Miao, and J. D. Palmer. 1999. Investigating deep phylogenetic relationships among cyanobacteria and plastids by small subunit rRNA sequences analysis. J. Eukaryot. Microbiol. **46**: 327–338. doi:10.1111/j.1550-7408.1999.tb04612.x.

Uchimiya, M., C. Motegi, S. Nishino, Y. Kawaguchi, J. Inoue, H. Ogawa, and T. Nagata. 2016. Coupled response of bacterial production to a wind-induced fall phytoplankton bloom and sediment resuspension in the Chukchi Sea Shelf, western Arctic Ocean. Front. Mar. Sci. **3**: 231. doi:10.3389/fmars.2016.00231.

Wang, F., R. W. Macdonald, D. A. Armstrong, and G. A. Stern. 2012. Total and methylated mercury in the Beaufort Sea: The role of local and recent organic remineralization. Environ. Sci. Technol. **46**: 11821–11828. doi:10.1021/es302882d.

Wang, K., K. M. Munson, A. Beaupré-Laperrière, A. Mucci, R. W. Macdonald, and F. Wang. 2018. Subsurface seawater methylmercury maximum explains biotic mercury concentrations in the Canadian Arctic. Sci. Rep. **8**: 14465. doi:10.1038/s41598-018-32760-0.

Wright, J. J., S. Lee, E. Zaikova, D. A. Walsh, and S. J. Hallam. 2009. DNA extraction from 0.22 μM Sterivex filters and cesium chloride density gradient centrifugation. J. Vis. Exp. **31**: 1352. doi:10.3791/1352.

Zheng, R., S. Wu, N. Ma, and C. Sun. 2018. Genetic and physiological adaptations of marine bacterium *Pseudomonas stutzeri* 273 to mercury stress. Front. Microbiol. **9**: 682. doi:10.3389/fmicb.2018.00682.

Acknowledgments

We thank Chief Scientists David Kadko and Bill Landing and the captain and crew of the USCGC *Healy*, and Jon Zehr, Mary Hogan, and Kendra Turk-Kubo of UCSC for access to and help in using the MEGAMER facility. We also thank the GEOTRACES in situ pump team (Phoebe Lam, Steve Pike, Yang Xiang, and Maija Heller) for aid in DNA collection and Ann Wymore of Oak Ridge National Laboratories for training on PCR using *hgcAB* primers. This work was funded by the National Science Foundation grants OCE-1434650, OCE-1434653, and OCE-1534315.

Conflict of Interest

None declared.

Submitted 28 January 2019
Revised 14 June 2019
Accepted 26 July 2019

Associate editor: David Walsh